

See discussions, stats, and author profiles for this publication at: <https://www.researchgate.net/publication/319087912>

# Genome downsizing, physiological novelty, and the global dominance of flowering plants

Article · August 2017

DOI: 10.1101/174615

---

CITATIONS

0

READS

69

2 authors:



[Kevin A Simonin](#)  
San Francisco State University  
31 PUBLICATIONS 899 CITATIONS

[SEE PROFILE](#)



[Adam B Roddy](#)  
Yale University  
24 PUBLICATIONS 128 CITATIONS

[SEE PROFILE](#)

Some of the authors of this publication are also working on these related projects:



Flower hydraulics [View project](#)



Leaf transpiration and isotopes [View project](#)

All content following this page was uploaded by [Kevin A Simonin](#) on 12 August 2017.

The user has requested enhancement of the downloaded file.

1    Genome downsizing, physiological novelty, and the global dominance of flowering  
2    plants

3

4    Kevin A. Simonin<sup>1\*</sup> and Adam B. Roddy<sup>2</sup>

5

6    <sup>1</sup>San Francisco State University, Department of Biology, San Francisco, CA, 94132, USA

7    <sup>2</sup>Yale University, School of Forestry and Environmental Studies, New Haven, CT, 06511,  
8    USA

9    \*Correspondence to: simonin@sfsu.edu

10

11    **Summary**

12

13    During the Cretaceous (145-66 Ma), early angiosperms rapidly diversified, eventually  
14    outcompeting the ferns and gymnosperms previously dominating most ecosystems.

15    Heightened competitive abilities of angiosperms are often attributed to higher rates of  
16    transpiration facilitating faster growth. This hypothesis does not explain how  
17    angiosperms were able to develop leaves with smaller, but densely packed stomata and  
18    highly branched venation networks needed to support increased gas exchange rates.

19    Although genome duplication and reorganization have likely facilitated angiosperm  
20    diversification, here we show that genome downsizing facilitated reductions in cell size  
21    necessary to construct leaves with a high density stomata and veins. Rapid genome  
22    downsizing during the early Cretaceous allowed angiosperms to push the frontiers of  
23    anatomical trait space. In contrast, during the same time period ferns and gymnosperms  
24    exhibited no such changes in genome size, stomatal size, or vein density. Further  
25    reinforcing the effect of genome downsizing on increased gas exchange rates, we found  
26    that species employing water-loss limiting crassulacean acid metabolism (CAM)  
27    photosynthesis, have significantly larger genomes than C3 and C4 species. By directly  
28    affecting cell size and gas exchange capacity, genome downsizing brought actual primary  
29    productivity closer to its maximum potential. These results suggest species with small  
30    genomes, exhibiting a larger range of final cell size, can more finely tune their leaf  
31    physiology to environmental conditions and inhabit a broader range of habitats.

32

33

34     **Introduction**

35         The abrupt origin and rapid diversification of the flowering plants during  
36         the mid-Cretaceous, and their eventual dominance globally, has long been  
37         considered an ‘abominable mystery’<sup>1</sup>. While the cause of their high diversity has  
38         been attributed primarily to coevolution with pollinators and herbivores, many  
39         hypotheses have been posed to explain why angiosperms were able to become  
40         ecologically dominant in most terrestrial ecosystems. A common theme among  
41         these hypotheses has been the idea that angiosperms developed a set of  
42         physiological traits that allowed them to achieve higher rates of primary  
43         productivity than either the ferns or the gymnosperms<sup>2</sup>. Terrestrial primary  
44         productivity is determined by the photosynthetic capacity of leaves, and one of  
45         the greatest biophysical limitations to photosynthetic rates across all the major  
46         clades of terrestrial plants is the leaf surface conductance to CO<sub>2</sub> and water vapor.  
47         In order for CO<sub>2</sub> to diffuse from the atmosphere into the leaf, the wet internal  
48         surfaces of leaves must be exposed to the dry ambient atmosphere, which can  
49         cause leaf desiccation and prevent further CO<sub>2</sub> uptake. As a consequence,  
50         increasing leaf surface conductance to CO<sub>2</sub> also requires increasing rates of leaf  
51         water transport in order to avoid desiccation<sup>3</sup>.

52         Both theory and empirical data suggest that among all major clades of  
53         terrestrial plants the upper limit of leaf surface conductance to CO<sub>2</sub> and water  
54         vapor is tightly coupled to biophysical limitations on cell size<sup>4-7</sup>. Cellular  
55         allometry, in particular the scaling of genome size, nuclear volume, and cell size  
56         represents a direct physical constraint on the number of cells that can occupy a

57 given space and, as a result, on the distance between cell types and tissues<sup>8</sup>.

58 Because leaves with many small stomata and a high density of veins promote

59 higher rates of gas exchange than leaves with fewer, larger stomata and larger,

60 less dense veins<sup>9</sup>, variation in cell size can drive large changes in potential carbon

61 gain<sup>10</sup>. Without reducing cell size, increasing stomatal and vein densities would

62 displace other important tissues, such as photosynthetic mesophyll cells<sup>11</sup>.

63 Therefore, the densities of stomata on the leaf surface and of veins inside the leaf

64 are inversely related to the sizes of guard cells and xylem elements of which they

65 are comprised.

66 While numerous environmental and physiological factors can influence

67 the final sizes of somatic eukaryotic cells, the minimum size of meristematic cells

68 and the rate of their production are strongly constrained by nuclear volume, more

69 commonly measured as genome size<sup>12-15</sup>. Among land plants, the bulk DNA

70 content of cells varies by three orders of magnitude, with the angiosperms

71 exhibiting both the largest range in genome size and the smallest absolute genome

72 sizes<sup>16</sup>. Whole-genome duplications and subsequent genomic rearrangements

73 rapidly change genome size and are thought to have directly contributed to the

74 unparalleled diversity in anatomical, morphological, and physiological traits of

75 the angiosperms<sup>15,17-21</sup>. We extend this prior work and predict that genome size

76 variation is not only responsible for gene diversification but also directly controls

77 minimum cell size and, thus, is the underlying variable directly influencing both

78 stomatal size and density and leaf vein density thus directly influencing rates of

79 leaf gas exchange across the major clades of terrestrial plants.

80 To test whether genome downsizing among the angiosperms drove the  
81 anatomical and physiological innovations that resulted in their ecological  
82 dominance over other major clades of terrestrial plants, we compiled data for  
83 genome size, cell size (guard cell length,  $l_g$ ), leaf vein density ( $D_v$ ), and maximum  
84 and operational leaf surface conductance to CO<sub>2</sub> and water vapor ( $g_{s,max}$  and  $g_{s,op}$ ,  
85 respectively) for almost 1100 species of ferns, gymnosperms, and angiosperms. If  
86 genome downsizing were critical for angiosperm success, then we expect genome  
87 size to have declined rapidly during early angiosperm evolution but, perhaps, to  
88 have remained unchanged among the ferns and gymnosperms. Furthermore, if  
89 genome size constrains  $l_g$  and  $D_v$ , then evolutionary changes in genome size  
90 should precede changes in both  $l_g$  and  $D_v$ . Finally, we predict that the benefits of  
91 genome downsizing on carbon gain should be greatest when photosynthesis and  
92 transpiration are proportional, such as in plant species that possess C3 and C4  
93 photosynthetic metabolism, in contrast to species employing crassulacean acid  
94 metabolism (CAM), which decouples gas exchange from periods of high  
95 evaporative demand. If these predictions about the biophysical effects of genome  
96 size and its evolution are supported, then genome downsizing among the  
97 angiosperms led directly to their greater potential and realized primary  
98 productivity, contributing to their rapid domination of ecosystems globally.

99

100 **Results**

101 *Trait correlations (genome vs vein density and cell size) and phylogenetic independent*  
102 *contrasts*

103        Genome size varied substantially among major clades (Figure 1) and was  
104        a strong predictor of anatomical traits across the major groups of terrestrial plants  
105        even when accounting for phylogeny. Genome size explained 42% of between  
106        species variation in  $l_g$  across the major groups of terrestrial plants (Figure 2a).  
107        Additionally, a single relationship predicted  $l_g$  from genome size across all  
108        species. Similarly, a strong negative correlation existed between genome size and  
109        both  $D_s$  (Figure 2b;  $R^2 = 0.32$ ) and  $D_v$  (Figure 2c;  $R^2 = 0.46$ ). Among major clades  
110        and within the angiosperms, traits showed strong, significant correlations between  
111        PICs, highlighting the coordinated evolution of these traits repeatedly throughout  
112        the history of seed plants (Table S2).

113

114        *Biophysical scaling relationships: maximum and operational leaf surface conductance*  
115        Within clades, only the angiosperms exhibited a significant relationship between  
116        genome size and either  $g_{s,\max}$  or  $g_{s,\text{op}}$ . Sample sizes among the ferns and gymnosperms for  
117        these traits were quite low, precluding statistical significance. Yet, ferns and  
118        gymnosperms fell within the ranges of  $g_{s,\max}$  and  $g_{s,\text{op}}$  defined by the angiosperms. The  
119        global scaling relationships among all species between genome size and either  $g_{s,\max}$  or  
120         $g_{s,\text{op}}$  were not significantly different than those for only the angiosperms, suggesting that a  
121        single relationship may exist between genome size and stomatal conductance (Figure 3).

122        Regardless of the leaf thickness (70, 100, 130  $\mu\text{m}$ ) used to calculate  $g_{s,\text{op}}$ , the  
123        scaling relationships between genome size and  $g_{s,\text{op}}$  were significantly steeper than the  
124        relationship between genome size and  $g_{s,\max}$  (all  $P < 0.001$ ). Therefore, across species,  
125        shrinking the genome brings  $g_{s,\text{op}}$  closer to  $g_{s,\max}$  (Figure 3, Table 1).

126

127 *Trait evolution through time*

128       Compared to the ferns and gymnosperms, genome sizes,  $D_v$ , and  $l_g$  of the  
129   angiosperms all evolved into new regions of trait space during the Cretaceous (Figure 4),  
130   increasing rates of carbon assimilation and ushering in more rapidly growing forests. For  
131   all three traits, the logarithmic curve fit the extreme values better than a linear  
132   relationship (genome size  $\Delta\text{AIC} = 12.89$ ;  $D_v \Delta\text{AIC} = 11.43$ ;  $l_g \Delta\text{AIC} = 24.69$ ). In contrast  
133   to the angiosperms, fern and gymnosperm lineages exhibited no such change in any of  
134   the traits during the Cretaceous. For fern and gymnosperm traits, the linear fit including a  
135   slope and intercept was not significantly better than the model lacking a slope (i.e. the  
136   mean reconstructed trait value), except for fern minimum  $l_g$ , which was better modeled by  
137   a linear regression with a slope, although this model indicated that fern  $l_g$  increased  
138   through time (Figure 4).

139       Genome size evolution among C3 species was best modeled by allowing for  
140   different rates of trait evolution for the three clades, consistent with our prediction that  
141   the angiosperms capitalized on genome downsizing. Although we had predicted that OU  
142   models, which model stabilizing selection around optimum trait values, would best fit the  
143   data, the best-fitting model was instead the Brownian motion model that included  
144   different rates for each clade. In this model, the rate parameter indicates the standard  
145   deviation of trait values around the phylogenetic mean; thus a faster rate is indicative of  
146   greater trait variance. In all 100 simulations, the Brownian motion model provided the  
147   best fit with  $\Delta\text{AIC} = 14.33 \pm 0.17$ , compared to the second-best fitting model in each  
148   iteration (Table 2). Across all C3 taxa, genome size evolved faster in the ferns ( $0.19 \pm$

149 0.0009) and gymnosperms ( $0.14 \pm 0.0008$ ) than in the angiosperms ( $0.088 \pm 0.0006$ ).  
150 Similarly, in the combined analysis that incorporated all clades and photosynthetic  
151 pathways, a Brownian motion model with multiple rates best described the data in all 100  
152 simulations ( $\Delta AIC = 130.14 \pm 1.20$ ), and the modeled parameters were similar to those  
153 from the other models (Table 2).

154 Among the angiosperms, genome size evolution differed with photosynthetic  
155 pathway, reflecting that genome size-cell size allometry imposes different constraints on  
156 C3 and CAM species (Figures 1, 5). First, genome size evolution was best modeled by a  
157 Brownian motion process (100 out of 100 simulations,  $\Delta AIC = 102.39 \pm 1.04$ ; Table 2)  
158 that allowed for multiple rates of evolution for lineages employing the different  
159 photosynthetic pathways. CAM lineages had the largest estimated phylogenetic mean  
160 genome size (equivalent to the estimated ancestral genome size) and also the fastest rate  
161 of genome size evolution, in both balanced (phylogenetic mean:  $t = 18.61$ ,  $df = 105.11$ ,  $P < 0.0001$ ; rate:  $t = 35.36$ ,  $df = 99.65$ ,  $P < 0.0001$ ) and unbalanced (phylogenetic mean:  $t = 30.89$ ,  $df = 113.66$ ,  $P < 0.0001$ ; rate:  $t = 47.53$ ,  $df = 100.99$ ,  $P < 0.0001$ ) species sampling  
163 (Figure 4). Second, we tested whether there were time lags between shifts in genome size  
164 and shifts in either  $D_v$  or  $l_g$  associated with transitions between photosynthetic pathways.  
165 If genome size fundamentally constrains  $D_v$  and  $l_g$ , then shifts in genome size should  
166 either coincide with or precede shifts in the other traits, but genome size should not lag  
167 behind either  $D_v$  or  $l_g$ . Although in 96 of 100 simulations vein density lagged behind  
169 genome size, support for this model was weak ( $\Delta AIC = 2.80 \pm 0.16$ ), suggesting that  
170 there has been little or no lag between  $D_v$  and genome size. Similarly, although shifts in  $l_g$   
171 lagged behind shifts in genome size in 80 of 100 simulations, support was weak ( $\Delta AIC =$

172    0.99 ± 0.09). In the other 20 simulations, there was no lag between shifts in genome size  
173    and  $l_g$  ( $\Delta AIC = 1.32 \pm 0.45$ ), further suggesting that genome size and cell size evolve in  
174    unison. In none of the time lag simulations did genome size lag behind either  $D_v$  or  $l_g$ ,  
175    strengthening support for genome size fundamentally constraining both  $l_g$  and  $D_v$ .

176

## 177    **Discussion**

178       Our results suggest that the basis for developing leaves with the potential  
179    for high rates of gas exchange derive not exclusively from common  
180    developmental programs nor from genetic correlations (i.e. linkage between genes  
181    controlling both traits), but, even more fundamentally, from biophysical scaling  
182    constraints that limit minimum cell size <sup>4,38</sup>. These scaling relationships between  
183    genome size and gas exchange rates as well as analyses of trait evolution suggest  
184    that genome downsizing among the angiosperms permitted the evolution of the  
185    anatomical traits responsible for increased rates of photosynthesis and biomass  
186    accumulation (Figures 2-4). Importantly, while genome downsizing has been  
187    critical to increasing leaf gas exchange rates among the angiosperms, it was not a  
188    key innovation that occurred only at the root of the angiosperm phylogeny.  
189       Rather, the angiosperms exhibit a wide range of genome sizes, and coordinated  
190    changes in genome size and physiological traits have repeatedly occurred  
191    throughout the evolutionary history of the angiosperms (Table S2). Whole-  
192    genome duplications have been particularly important in promoting  
193    diversification among the angiosperms <sup>17</sup> yet result in larger, physiologically

194 detrimental, genomes. Our results suggest that genome downsizing is critical to  
195 recovering leaf gas exchange capacity subsequent to genome duplications.

196 The ecological revolution ushered in by the angiosperms is due largely to  
197 the biophysical benefits associated with decreasing genome and cell sizes. If  
198 heightened competitive ability among the angiosperms drove their ecological  
199 dominance, then innovations that allowed minimum cell size to decline were  
200 critical to this transformative process <sup>38</sup>. Because genome size provides a  
201 boundary on minimum cell size, genome size has numerous consequences for the  
202 structure and organization of cells and tissues in leaves, which directly influence  
203 metabolic rates. Specifically, unlike ferns and gymnosperms, angiosperms were  
204 able to develop leaves with numerous, small stomata and a high density of veins  
205 because of rapid reductions in genome size during the Cretaceous (Figures 2, 4).  
206 Non-angiosperm lineages exhibited no similar changes in these traits during the  
207 same time, despite a single, universal scaling relationship in all major clades of  
208 terrestrial plants between genome size and anatomical ( $D_v$  and  $l_g$ ) and  
209 physiological ( $g_{s,max}$  and  $g_{s,op}$ ) traits. Across seed plants, genome downsizing  
210 effectively brings actual productivity closer to its theoretical maximum (Figure 3),  
211 allowing the angiosperms to outcompete other land plants.

212 Cell size has direct and predictable effects on gas diffusion across the leaf  
213 epidermis, and, as we show here, also on the supply of liquid water to the leaf.  
214 Physical resistance to diffusion across leaf surfaces is ultimately determined by  
215 the size of epidermal cells, and the maximum diffusive conductance of CO<sub>2</sub> and  
216 water vapor ( $g_{s,max}$ ) is higher in leaves with numerous, small stomata <sup>4,6,7</sup>. While

217 the effects of cell size on leaf epidermal properties have been well characterized,  
218 the effects of cell size on the efficiency of liquid water supply through the leaf  
219 are, perhaps, less obvious. Given a constant leaf volume, increasing  $D_v$  without  
220 displacing photosynthetic mesophyll cells requires reductions in vein and conduit  
221 sizes that can only be accomplished by decreasing cell size<sup>11,39</sup>. However, smaller  
222 conduits have higher hydraulic resistances. To overcome the increase in resistance  
223 associated with reducing conduit sizes, other innovations in xylem anatomy that  
224 reduce hydraulic resistance have been hypothesized to facilitate narrower xylem  
225 conduits and high  $D_v$ . In particular, the development of low resistance end walls  
226 between adjacent cells is thought to have given angiosperms a hydraulic  
227 advantage as conduit diameters decreased. Only in angiosperm lineages with very  
228 high  $D_v$  do primary xylem have simple perforation plates, which have lower  
229 resistance to water flow than scalariform perforation plates<sup>11</sup>. Similarly, the low  
230 resistance of gymnosperm torus-margo pits compared to angiosperm pits can  
231 result in higher xylem specific hydraulic conductivity for small diameter conduits  
232<sup>40</sup>. In both cases, while smaller conduits have higher resistance, this potential cost  
233 has been offset by other innovations that reduce hydraulic resistance at the scale  
234 of the whole xylem network. The requirement of these other changes to xylem  
235 anatomy to occur before potential gains from reduced conduit sizes can be  
236 realized may explain why evolutionary shifts in  $D_v$  almost always lagged behind  
237 shifts in genome size associated with transitions between photosynthetic  
238 pathways. In contrast, shifts in  $l_g$  were less likely to lag behind shifts in genome

239 size, instead evolving concurrently with genome size, probably due to the direct  
240 and simple effect of genome size on  $l_g$  without the need for other traits to evolve.

241 While genome size limits minimum cell size, final cell size can vary  
242 greatly as cells grow and differentiate. After cell division and during cell  
243 expansion, various factors influence how large a cell becomes. Intracellular turgor  
244 pressure overcomes the mechanical rigidity of the cell wall to enlarge cellular  
245 boundaries. The magnitude of turgor pressure is itself controlled by water  
246 availability around the cell and the osmotic potential inside the cell. Final cell size  
247 is controlled therefore by both biotic and abiotic factors that influence pressure  
248 gradients in and around the cell. By reducing the lower limit of cell size, genome  
249 downsizing expands the range of final cell size that is possible. Thus, species that  
250 can vary cell size across a wider range can more finely tune their leaf anatomy to  
251 match environmental constraints on leaf gas exchange. Indeed,  $D_v$ ,  $l_g$ , and  
252 stomatal conductance are more variable among species with small genomes, and  
253 the variance in these traits unexplained by genome size is likely due to  
254 environmental variation (Figures 2-4), although analyses of intraspecific genome  
255 size variation are needed to further clarify the potential links between genome size  
256 variation and environmental variation. Interestingly, only the angiosperms occupy  
257 this region of trait space, and the angiosperms tend to be more productive than  
258 either the ferns or the gymnosperms across a broad range of environmental  
259 conditions. Furthermore, genome size may predict ecological breadth even within  
260 species insofar as species with small genomes can exhibit greater plasticity in  
261 final cell size and inhabit a wider range of environmental conditions. Thus, rapid

262 genome downsizing by the angiosperms during the Cretaceous likely explains not  
263 only their greater potential and realized primary productivity (Figure 3) but also  
264 why they were able to expand into and create new ecological habitats,  
265 fundamentally altering the global biosphere and atmosphere<sup>41</sup>.

266 Yet, not all angiosperms have small genomes (Figures 1-2). Genome size-  
267 cell size allometry determines physiological function within a given environment  
268 when photosynthetic rates are proportional to transpiration rates. This is certainly  
269 the case for species employing the C3 and C4 photosynthetic pathways. However,  
270 due to higher water use efficiency of C4 photosynthesis, the physiological effects  
271 of genome size variation may be slightly weaker in C4 species than they are in C3  
272 species, as reflected in the slightly larger genomes and guard cell lengths of C4  
273 species. Nonetheless,  $D_v$  and photosynthetic metabolism in many C4 plants are  
274 intimately linked due to the physical arrangement of the sites of carboxylation  
275 into a layer of cells surrounding the veins (i.e. bundle sheath cells). Because of  
276 this physical association, increasing the number of cells that are able to assimilate  
277 CO<sub>2</sub> requires an increase in the number of veins. In contrast to both C3 and C4  
278 photosynthetic metabolism, species employing CAM photosynthesis effectively  
279 decouple carbon uptake from periods of relatively high evaporative demand. For  
280 CAM species, the constraints of genome size on the coordination between carbon  
281 gain and water loss are minimal, and, as a result, CAM species have significantly  
282 larger genomes than either C3 or C4 species (Figures 4-5). CAM lineages also  
283 have faster rates of genome size evolution than C3 lineages, suggesting that  
284 genome size may be more constrained in C3 lineages because cell size has a direct

285 and substantial effect on gas exchange rates (Figure 5). However, the limited  
286 taxonomic resolution of CAM photosynthesis may be biasing our estimates of  
287 evolutionary rates. There are undoubtedly C3 species and C3-CAM intermediates  
288 that we have classified as strictly CAM, which would increase the disparity in  
289 genome size and lead to an underestimation of the difference in genome size  
290 between C3 and CAM species but an overestimation of the rate of genome size  
291 evolution among species classified as strictly CAM. Nonetheless, the difference in  
292 genome size between extant C3 and CAM species highlights the fundamental  
293 importance of genome downsizing in raising the limits of leaf gas exchange when  
294 carbon uptake is directly coupled to water loss. By no means should this trivialize  
295 the ecological importance of CAM photosynthesis. Rather, it reinforces the  
296 innovativeness of the angiosperms because genome downsizing is not the only  
297 strategy conferring ecological success; CAM photosynthesis, regardless of  
298 genome size, has allowed colonization of marginal environments often  
299 uninhabitable by C3 species.

300

301 **Conclusion**

302 The rapid diversification and spread of angiosperms during the Cretaceous  
303 dramatically restructured terrestrial ecosystems<sup>41,42</sup>. While their heightened  
304 diversification rates have long been thought to result from a combination of  
305 unique traits that allowed them to coevolve with pollinators and herbivores<sup>43-47</sup>,  
306 only recently have hypotheses about how angiosperms became ecologically  
307 dominant been considered. Central to these hypotheses has been that the

308 angiosperms became competitively more successful due to faster growth rates<sup>48</sup>,  
309 supported by higher rates of photosynthesis and transpiration<sup>9,30,42</sup>. Anatomical  
310 innovations that appeared among the angiosperms—smaller, more abundant  
311 stomata and narrower, more densely packed leaf veins—that support higher rates of  
312 transpiration and photosynthesis would have been particularly advantageous as  
313 atmospheric CO<sub>2</sub> concentration declined during the Cretaceous. These traits are  
314 unique to the angiosperms and due, we show, to reductions in cell and genome  
315 sizes that occurred after the appearance of early angiosperms. Smaller genomes  
316 and cells increased leaf surface conductance to CO<sub>2</sub> and enabled higher potential  
317 and realized primary productivity. Interestingly, the physiological benefits of  
318 small genomes and cells are realized only when photosynthetic rates are  
319 proportional to transpiration rates; species employing CAM photosynthesis avoid  
320 assimilating CO<sub>2</sub> during periods of high evaporative demand driven by light  
321 interception. As a result, CAM species can have larger genomes without the  
322 physiological costs that C3 species might incur. Additionally, CAM species often  
323 inhabit marginal habitats characterized by limited water availability and nutrient  
324 cycling that are unable to support high rates of primary productivity<sup>49</sup>.  
325 Furthermore, because genome downsizing lowers the limit of minimum cell size,  
326 final cell size can vary much more widely, which facilitates a closer coupling of  
327 anatomy and physiology with environmental conditions. Therefore, genome  
328 downsizing has increased the range of habitable environments and allowed  
329 angiosperms to outcompete other land plants in almost every ecosystem.  
330

331   **Methods**

332

333   *Leaf traits*

334   Published data for guard cell length ( $l_g$ ), stomatal density ( $D_s$ ), and vein density  
335   ( $D_v$ ) were compiled from the literature (Table S1). Genome size data for each  
336   species were taken from the Plant DNA C-values database (release 6.0, December  
337   2012), managed by the Royal Botanic Gardens, Kew <sup>22</sup>. In total, our dataset  
338   comprised 1087 species of vascular plants, of which 979 were angiosperms, 54  
339   were gymnosperms, and 54 were ferns. For the 979 angiosperms in the dataset,  
340   there were  $D_v$  data for 164 and guard cell size data for 220. Similarly, there were  
341    $D_v$  data for 23 gymnosperms and for 10 ferns, and there were  $l_g$  data for 20  
342   gymnosperms and for 41 ferns. The large discrepancy between the total number  
343   of angiosperms in the dataset and the number of angiosperms with leaf trait data is  
344   due to inclusion of genome size data for CAM species that lacked leaf trait data.

345       Because different photosynthetic pathways (C3, C4, CAM) employ different  
346   strategies of maintaining water balance, the effects of genome size-cell size allometry  
347   may differ among species employing different photosynthetic pathways. We tested this  
348   hypothesis by comparing genome size evolution among the angiosperms. We expected  
349   the largest difference to exist between C3 and CAM species, and so we focused the  
350   analysis on this comparison. The taxonomic distribution of CAM photosynthesis was  
351   based on Smith and Winter <sup>23</sup>, which provides a list of genera exhibiting CAM  
352   photosynthesis. Undoubtedly, some of these genera include C3 species (either C3-CAM  
353   intermediates or exclusively C3), which would lead to a conservative estimate of the

354 differences in genome size between C3 and CAM species. Of the 973 angiosperms in this  
355 analysis, 271 were C3, nine were C4, and 647 were CAM.

356

357 *Calculating maximum and operational stomatal conductance*

358 For each species in our database with anatomical traits, we calculated the maximum  
359 stomatal conductance and the operational stomatal conductance. Maximum stomatal  
360 conductance ( $g_{s,\max}$ ) is defined by the dimensions of stomatal pores and their abundance,  
361 and represents the biophysical upper limit of gas diffusion through the leaf epidermis.

362 Anatomical measurements of guard cells were used to calculate  $g_{s,\max}$  as<sup>4,5</sup>:

363

$$364 \quad g_{s,\max} = \frac{D_s \cdot a_{\max} \cdot m_v}{d_p + \frac{\pi}{2} \sqrt{a_{\max}/\pi}} \quad (1)$$

365

366 where  $d_{H_2O}$  is the diffusivity of water in air (0.0000249 m<sup>2</sup> s<sup>-1</sup>),  $m_v$  is the molar volume of  
367 air normalized to 25 °C (0.0224 m<sup>3</sup> mol<sup>-1</sup>),  $D_s$  is stomatal density (mm<sup>-2</sup>),  $a_{\max}$  is  
368 maximum stomatal pore size, and  $d_p$  is the depth of the stomatal pore. The  $a_{\max}$  term can  
369 be approximated as:  $\pi(l_p/2)^2$ , where  $l_p$  is stomatal pore length with  $l_p$  being approximated  
370 as  $l_g/2$ , where  $l_g$  is guard cell length<sup>4,24</sup>.  $d_p$  is assumed to be equal to guard cell width ( $W$ ).  
371 If  $W$  was not reported  $d_p$  was estimated as  $0.36 \cdot l_g$ <sup>7</sup>.

372 Operational stomatal conductance ( $g_{s,op}$ ), by contrast, more accurately defines the  
373 stomatal conductance leaves attain under natural conditions when limitations in leaf  
374 hydraulic supply constrain stomatal conductance. We used an empirical model of  $g_{s,op}$ <sup>3</sup>  
375 that directly relates  $D_v$  to stomatal conductance during periods of steady state  
376 transpiration as:

377

378  $K_{\text{leaf}} = 12,670d_m^{-1.27}$  (2)

379 where:

380  $d_m = \pi/2(d_x^2 + d_y^2)^{1/2}$  (3)

381

382  $d_x = 650/D_v$  (4)

383

384  $g_{s, \text{op}} = (K_{\text{leaf}} \Delta\Psi)/v$  (5).

385

386  $K_{\text{leaf}}$  is leaf hydraulic conductance ( $\text{mmol m}^{-2} \text{ s}^{-1} \text{ MPa}^{-1}$ ),  $d_m$  is the post vein distance to  
387 stomata ( $\mu\text{m}$ ),  $d_x$  is the maximum horizontal distance from vein to the stomata ( $\mu\text{m}$ ),  $d_y$  is  
388 the distance from vein to the epidermis ( $\mu\text{m}$ ),  $\Delta\Psi$  is the water potential difference  
389 between stem and leaf (set to 0.33 MPa<sup>25</sup>) and  $v$  is vapor pressure deficit set to 2 kPa. In  
390 order to test the influence of variation in leaf thickness on  $g_{s, \text{op}}$  we used three values of  $d_y$   
391 (70, 100 and 130  $\mu\text{m}$ ).

392

393 *Analyses of trait evolution*

394 To determine the temporal patterns of trait evolution, we generated a phylogeny  
395 from the list of taxa (Table S1) using Phylomatic (v. 3) and its stored family-level  
396 supertree (v. R20120829). To date nodes in the supertree, we compiled node ages from  
397 recent, fossil-calibrated estimates of crown group ages. Node ages were taken from  
398 Magallón et al.<sup>26</sup> for angiosperms, Lu et al.<sup>27</sup> for gymnosperms, and Testo and Sundue<sup>28</sup>  
399 for ferns. The age of all seed plants was taken as 330 million years<sup>29</sup>. Because there is

400 some uncertainty in the maximum age of the ancestor of all angiosperms, we took the  
401 angiosperm crown age used by Brodribb and Field<sup>30</sup> to make our results directly  
402 comparable to theirs. We tested this assumed angiosperm age by using different ages for  
403 the crown group angiosperms ranging from 130 Ma to 180 Ma, and the results were not  
404 qualitatively different. Of the 331 internal nodes in our tree, 90 of them had ages. These  
405 ages were assigned to nodes and all other branch lengths smoothed using the function  
406 ‘bladj’ in the software Phylocom (v. 4.2<sup>31</sup>). Polytomies were resolved by random  
407 bifurcation and adding 5 million years to each of these new branches and subtracting an  
408 equivalent amount from the descending branches so that the tree remained ultrametric.  
409 For all subsequent analyses of character evolution, this method for randomly resolving  
410 polytomies was repeated 100 times to account for phylogenetic uncertainty. To fit models  
411 of trait evolution, stochastic character change<sup>32</sup> was mapped on each randomly resolved  
412 tree using the function ‘make.simmap’ in the R package *phytools*<sup>33</sup> before fitting each  
413 model of evolution (described below). For ancestral state reconstructions the ages and  
414 character estimates at each node were averaged across the 100 randomly resolved trees.

415 Ancestral state reconstructions were calculated using the residual maximum  
416 likelihood method, implemented in the function ‘ace’ from the R package *ape*<sup>34</sup>. To  
417 determine when changes in traits pushed the frontiers of trait values, the upper ( $D_v$ ) and  
418 lower (genome size and  $l_g$ ) limits of traits were estimated by first extracting the upper or  
419 lower ten percent of reconstructed trait values in sequential five million year windows  
420 and then attempting to fit curves to these values. This method is similar to a previous  
421 analysis of  $D_v$  evolution through time<sup>35</sup>, which is included here for comparison. We  
422 compared three types of curve fits: a linear fit that lacked slope (equivalent to the mean of

423 the reconstructed trait values), a linear fit that included both a slope and an intercept, and  
424 a nonlinear curve of the form  $trait = a + b/(1 + e^{-(time + c)/d})$ . Curves were fit to  
425 reconstructed trait values for each clade between 160 and 50 Ma, which corresponds to  
426 the time period encompassing the major diversification and expansion of the  
427 angiosperms, and the best fit was chosen based on AIC scores with a difference in AIC of  
428 5 taken to indicate significant differences in fits. Ancestral state reconstructions of  
429 genome size for CAM angiosperms were calculated separately from C3 and C4  
430 angiosperms because of the computational time required for the analyses. Phylogenetic  
431 independent contrasts (PICs) were used to determine whether traits underwent correlated  
432 evolution. PICs for each pairwise combination of traits were calculated for only species  
433 with data for both traits. Correlations between PICs were calculated using Spearman rank  
434 correlations in the function ‘cor.table’ from the R package *picante*<sup>36</sup>.

435 To determine whether the tempo and mode of genome size evolution differed  
436 among major clades and lineages with different photosynthetic pathways, we used the R  
437 package *mvMORPH*<sup>37</sup> to fit four types of evolutionary models under a maximum  
438 likelihood criterion: Brownian motion (BM) with a single rate of evolution for the entire  
439 tree, Brownian motion with multiple rates for different groups of taxa, Ornstein-  
440 Uhlenbeck (OU) process with a single adaptive optimum for all species, Ornstein-  
441 Uhlenbeck process with different trait optima for different groups of taxa. Three types of  
442 regimes were modeled: (1) C3 species in all three major clades, (2) angiosperms differing  
443 in photosynthetic pathway, (3) all clades and all photosynthetic pathways. In all of these  
444 analyses, we accounted for phylogenetic uncertainty as described above. Model fits were  
445 compared using AIC scores with a difference in AIC of 5 assumed to indicate a

446 significantly better model. In determining whether genome size evolution differed among  
447 angiosperms with different photosynthetic pathways, we attempted to account for the  
448 large discrepancy in the number of C3 and CAM angiosperms in the dataset by using all  
449 species ('unbalanced' analysis) and by randomly sampling 271 CAM species so that there  
450 were equivalent numbers of C3 and CAM species ('balanced' analysis). Then the same  
451 models as above were fit and compared. Because the analysis focused on the comparison  
452 between C3 and CAM species, *t*-tests were used to compare phylogenetic means and  
453 rates of genome size evolution, although estimated parameters for C4 species are  
454 included for completeness.

455 To determine whether there were temporal lags between changes in genome size  
456 and changes in  $D_v$  and  $l_g$ , we compared OU models that allowed for multiple trait optima  
457 that used symmetric (no time lag) and non-symmetric (one trait lags behind another)  
458 alpha matrices. Although in univariate analyses the OU model underperformed the BM  
459 models, analyses of time lags between trait shifts can be assessed using only OU models.  
460

#### 461 *Scaling relationships*

462 Scaling relationships between genome size and  $D_v$ ,  $l_g$ ,  $g_{s,max}$ , and  $g_{s,op}$  were  
463 calculated from log-transformed data and analyzed using the function 'sma' in the R  
464 package *smatr*<sup>36</sup>. Analyses were performed for the entire dataset and also for individual  
465 clades. Slope tests were used to determine whether the scaling relationship between  
466 genome size and  $g_{s,max}$  was significantly different than the relationship between genome  
467 size and  $g_{s,op}$  and whether the scaling relationship between genome size and  $g_{s,op}$  and  $g_{s,max}$   
468 differed among clades.

469 Figure 1. The distribution of genome size among 1035 land plants. The family level  
470 phylogeny has branches colored according to one random stochastic character map of  
471 photosynthetic pathways (C3, C4, CAM) among clades (ferns, gymnosperms,  
472 angiosperms). Orange bars at the tips are scaled proportional to genome size for each  
473 terminal species.

474

475 Figure 2. Relationships between genome size and anatomical traits: (a)  $l_g$ , (b)  $D_s$ , and (c)  
476  $D_v$ . In all panels, insets show log-log relationships and  $R^2$  values are from standard major  
477 axis regressions. Correlations for phylogenetically corrected relationships are in Table  
478 S2.

479

480 Figure 3. The relationships between genome size and maximum (solid line;  $R^2 = 0.25$ )  
481 and operational (dashed lines) stomatal conductance, plotted on a log-log scale.  
482 Operational stomatal conductance was modeled under assumptions of three leaf  
483 thicknesses (70  $\mu\text{m}$ ,  $R^2 = 0.46$ ; 100  $\mu\text{m}$ ,  $R^2 = 0.44$ ; 130  $\mu\text{m}$ ,  $R^2 = 0.43$ ). Points are  
484 omitted for clarity. Correlations for phylogenetically corrected relationships are in Table  
485 S2.

486

487 Figure 4. Ancestral state reconstructions of genome size, vein density ( $D_v$ ), and guard  
488 cell length ( $l_g$ ) through time for angiosperms (colored circles), gymnosperms (grey  
489 triangles), and ferns (grey squares). Error bars around reconstructed values represent  
490 error due to phylogenetic uncertainty. The shaded timespan indicates the Cretaceous,  
491 during which most major lineages of angiosperms diversified. Lines represent the best-fit

492 models through the lower (genome size and  $l_g$ ) and upper ( $D_v$ ) 10% of reconstructed  
493 values. (a) Genome size was unchanged during the Cretaceous for the ferns (genome size  
494 = 9.91, df = 2, P < 0.001) and the gymnosperms (genome size = 19.62, df = 2, P < 0.001),  
495 while minimum genome size among the angiosperms decreased rapidly during the  
496 Cretaceous (genome size =  $0.99 + 3.06/(1 + e^{-(time - 120.74)/9.03}; df = 5, P < 0.001)$ ).  
497 (b) Similar to the results of Brodribb and Field (2010), the upper limit of reconstructed  $D_v$   
498 through time increased significantly for the angiosperms ( $D_v = 3.93 + 5.29/(1 + e^{-(time$   
499  $- 124.47)/(-13.49)}); df = 5, P < 0.001$ ). However, vein densities of fern ( $D_v = 1.70; df = 2,$   
500 P < 0.01) and gymnosperm lineages ( $D_v = 1.68; df = 2, P < 0.001$ ) remained unchanged  
501 during the same time period. (c) Similarly,  $l_g$  declined rapidly among angiosperms ( $l_g =$   
502  $23.64 + 13.82/(1 + e^{-(time - 118.48)/9.31}); df = 5, P < 0.001$ ), while  $l_g$  of ferns ( $l_g =$   
503 42.52, df = 2, P < 0.001) and gymnosperms ( $l_g = 55.66, df = 2, P < 0.001$ ) remained  
504 unchanged during the Cretaceous. Marginal plots on the right represent the median  
505 (points), interquartile ranges (solid lines) and ranges (dotted lines) of extant trait values.  
506 Angiosperm data have been plotted separately for species exhibiting each photosynthetic  
507 pathway. The two CAM gymnosperms were included with C3 gymnosperms in these  
508 analyses.

509  
510 Figure 5. Differences in reconstructed genome size and the rate of genome size evolution  
511 for angiosperms differing in photosynthetic pathway. The reconstructed genome size and  
512 the rate of genome size evolution differed among C3 and CAM species, regardless of  
513 whether equivalent numbers of C3 and CAM species ('balanced', 271 species each) were  
514 randomly sampled or whether all CAM species were included in the analysis

515 ('unbalanced'). The rate of genome size evolution is the Brownian motion rate parameter  
516 calculated separately for each photosynthetic pathway. Points are medians, solid lines are  
517 interquartile ranges, and dotted lines are ranges of modeled parameters.

518  
519

Figure 1.

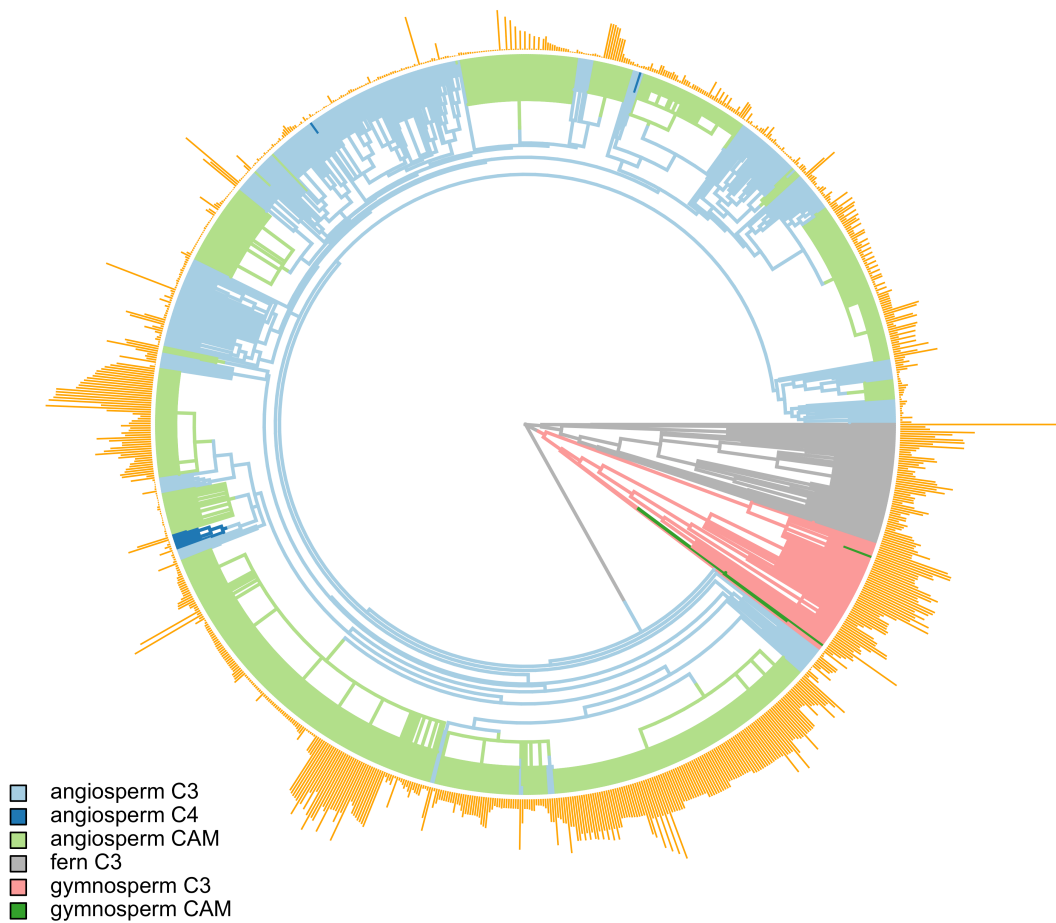


Figure 2.

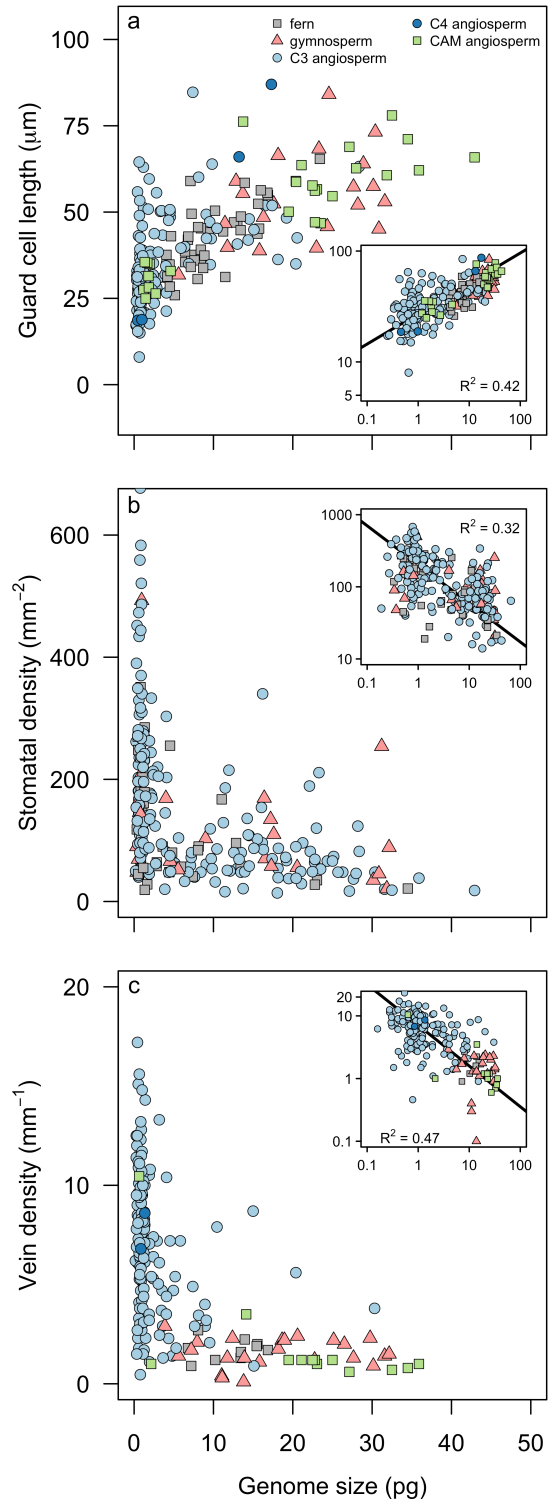


Figure 3.

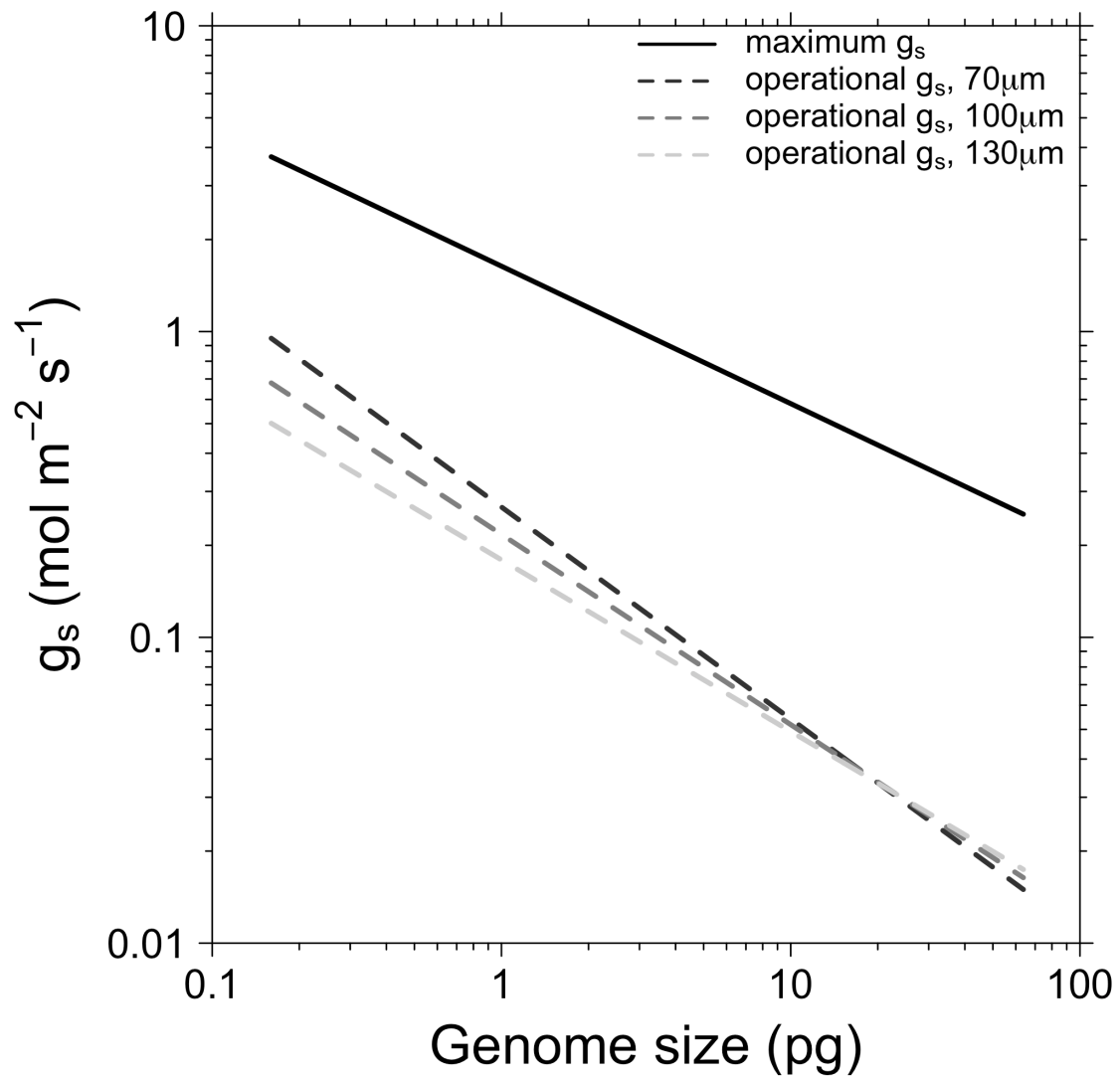


Figure 4.

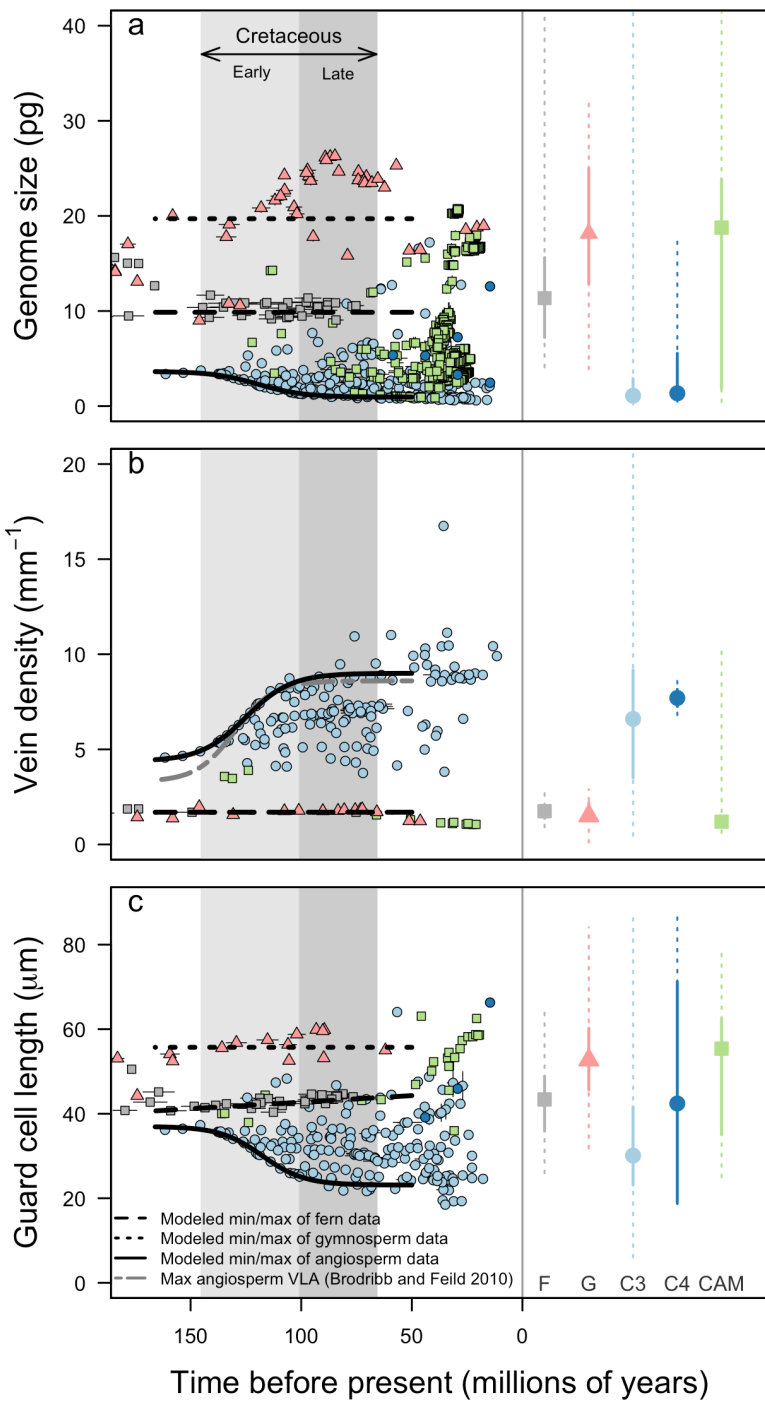


Figure 5.

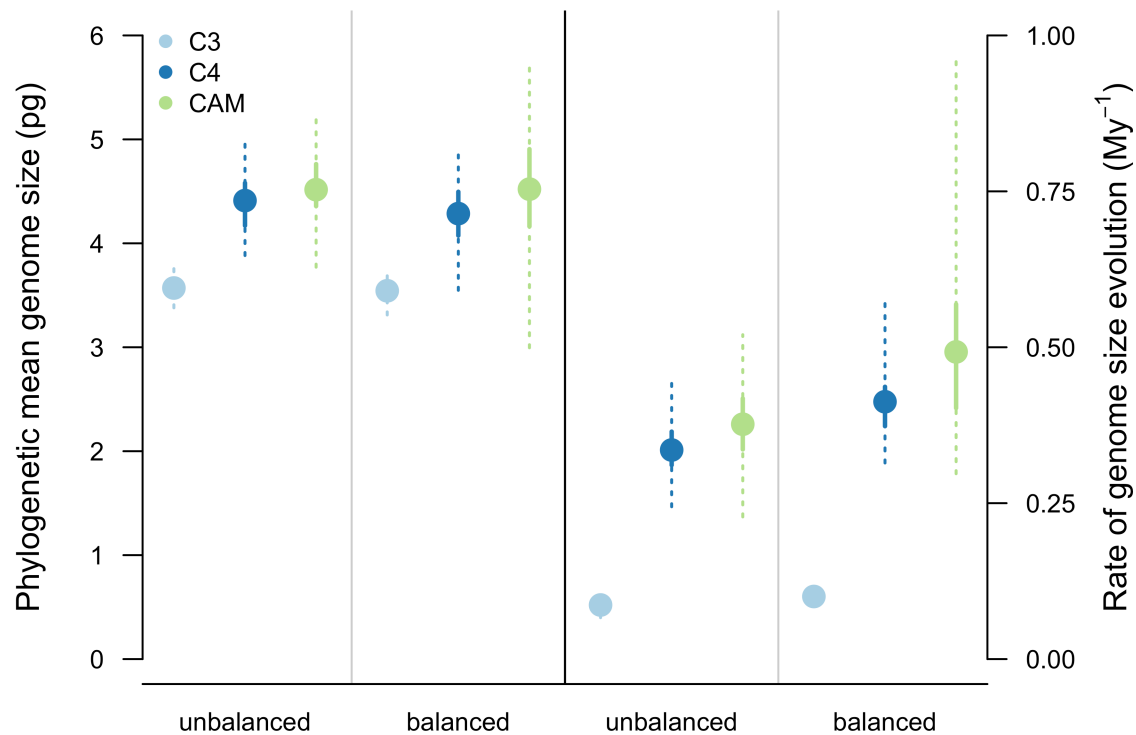


Table 1. Standard major axis regressions of  $D_v$ ,  $l_g$ ,  $g_{s,\max}$ , and  $g_{s,\text{op}}$  versus genome size for all species and for each clade separately. Asterisks indicate significance level: \* $P < 0.05$ ; \*\* $P < 0.01$ ; \*\*\* $P < 0.001$

	all			angiosperm			gymnosperm			fern		
	slope	intercept	R <sup>2</sup>	slope	intercept	R <sup>2</sup>	slope	intercept	R <sup>2</sup>	slope	intercept	R <sup>2</sup>
$D_v$	-0.646 (-0.716, -0.583)	0.848 (0.799, 0.897)	0.463 ***	-0.641 (-0.727, -0.566)	0.838 (0.789, 0.887)	0.329 ***	1.34 (0.864, 2.078)	-1.488 (-2.244, -0.732)	0.002	0.940 (0.454, 1.944)	-0.778 (-1.580, 0.025)	0.054
$l_g$	0.274 (0.249, 0.301)	1.435 (1.414, 1.456)	0.420 ***	0.300 (0.270, 0.333)	1.433 (1.411, 1.454)	0.477 ***	0.529 (0.354, 0.792)	1.036 (0.749, 1.324)	0.300	0.480 * (0.383, 0.602)	1.167 (1.060, 1.274)	0.523 ***
$g_{s,\max}$	-0.449 (-0.509, -0.397)	0.214 (0.167, 0.260)	0.245 ***	-0.447 (-0.514, -0.388)	0.208 (0.160, 0.255)	0.170 ***	1.178 (0.668, 2.078)	-1.750 (-2.646, - 0.854)	0.004	0.971 (0.425, 2.221)	-1.201 (-2.11, -0.288)	0.352
$g_{s,\text{op}}$ 70 $\mu\text{m}$	-0.693 (-0.769, -0.625)	-0.573 (-0.626, -0.522)	0.457 ***	-0.662 (-0.750, -0.584)	-0.586 (- 0.635, - 0.536)	0.335 ***	1.605 (1.010, 2.551)	-3.295 (-4.252, - 2.338)	0.001	1.169 (0.566, 2.415)	-2.473 (-3.468, -1.479)	0.060

Table 2. Univariate evolutionary modeling of genome size was best fit by a Brownian motion model with multiple rates. Parameter values are means  $\pm$  standard error of 100 replicate simulations accounting for phylogenetic uncertainty.  $\theta$  = genome size at the phylogenetic root,  $\sigma^2$  = rate of evolution.

Angiosperms: genome size							
	$\theta$	$\sigma^2$		Log-likelihood	AIC	Delta(AIC)	
C3	3.57 $\pm$ 0.008	0.087 $\pm$ 0.0006		-2749.6 $\pm$ 1.73	5511.2 $\pm$ 3.47	102.39 $\pm$ 1.04	
C4	4.39 $\pm$ 0.03	0.339 $\pm$ 0.0004					
CAM	4.52 $\pm$ 0.03	0.380 $\pm$ 0.006					
All clades: genome size							
Ferns	20.33 $\pm$ 0.009	0.194 $\pm$ 0.0009		-1074.2 $\pm$ 0.32	2160.4 $\pm$ 0.64	14.34 $\pm$ 0.17	
Gymnosperms	15.17 $\pm$ 0.008	0.140 $\pm$ 0.0008					
Angiosperms	3.53 $\pm$ 0.005	0.088 $\pm$ 0.0006					
All clades and pathways: Genome size							
Ferns	20.35 $\pm$ 0.008	0.194 $\pm$ 0.001		-3102.92 $\pm$ 1.771	6229.84 $\pm$ 3.542	130.14 $\pm$ 1.20	
C3 Gymnosperms	15.00 $\pm$ 0.008	0.136 $\pm$ 0.001					
CAM Gymnosperms	15.12 $\pm$ 0.030	0.0005 $\pm$ 0.0005					
C3	3.58 $\pm$	0.087 $\pm$					

angiosperms	0.009	0.001					
C4 angiosperms	$4.33 \pm 0.031$	$0.341 \pm 0.004$					
CAM angiosperms	$4.52 \pm 0.031$	$0.380 \pm 0.006$					

Table S2. Trait and phylogenetic independent contrast (PIC) correlations for all species and for only the angiosperms. Trait correlations are in the upper triangle and contrast correlations in the lower triangle. Spearman rank correlation coefficients are shown. Asterisks indicate significance level: \*P < 0.05; \*\*P < 0.01; \*\*\*P < 0.001

All species					
	Genome size	$D_v$	$I_g$	$g_{s, max}$	$g_{s, op 70}$
Genome size		-0.65***	0.74***	-0.46***	-0.65***
$D_v$	-0.16*		-0.63***	0.67***	0.99***
$I_g$	0.46***	-0.25*		-0.31***	-0.63***
$g_{s, max}$	-0.15*	0.35**	0.01		0.67***
$g_{s, op 70}$	-0.19**	0.99***	-0.25*	0.37**	
Angiosperms					
Genome size		-0.48***	0.65***	-0.34***	-0.49***
$D_v$	-0.16*		-0.56***	0.59***	0.99***
$I_g$	0.45***	-0.22		-0.23***	-0.56***
$g_{s, max}$	-0.17*	0.32*	0.04		0.59***
$g_{s, op 70}$	-0.19*	0.99***	-0.22	0.35**	

**Table S1 References**

1. Ahmad, K., Khan, M. A., Ahmad, M. & Zafar, M. Taxonomic diversity of stomata in dicot flora of a district tank (N.W.F.P.) in Pakistan. *African journal of ...* **8**, 1052–1055 (2009).
2. Álvarez, S. G., Amorena, I. G., Rubiales, J. M. & Morla, C. The value of leaf cuticle characteristics in the identification and classification of Iberian Mediterranean members of the genus *Pinus*. *Botanical Journal of the Linnean Society* **161**, 436–448 (2009).
3. Barrington, D. S., Paris, C. A. & Ranker, T. A. Systematic inferences from spore and stomate size in the ferns. *American Fern Journal* **76**, 149–159 (1986).
4. Beaulieu, J. M., Leitch, I. J., Patel, S., Pendharkar, A. & Knight, C. A. Genome size is a strong predictor of cell size and stomatal density in angiosperms. *New Phytologist* **179**, 975–986 (2008).
5. Blonder, B. & Enquist, B. J. Inferring climate from angiosperm leaf venation networks. *New Phytologist* **204**, 116–126 (2014).
6. Blonder, B., Violle, C., Bentley, L. P. & Enquist, B. J. Venation networks and the origin of the leaf economics spectrum. *Ecol Lett* **14**, 91–100 (2010).
7. Boyce, C. K., Brodribb, T. J., Feild, T. S. & Zwieniecki, M. A. Angiosperm leaf vein evolution was physiologically and environmentally transformative. *P R Soc B* **276**, 1771–1776 (2009).
8. Walls, R. Angiosperm leaf vein patterns are linked to leaf functions in a global-scale data set. *American Journal of Botany* **98**, 244–253 (2011).
9. Zonneveld, B. J. M. & Lindström, A. J. Genome sizes for 71 species of *Zamia*(Cycadales: Zamiaceae) correspond with three different biogeographic regions. *Nordic Journal of Botany* **34**, 744–751 (2016).
10. Carpenter, S. B. & Smith, N. D. Stomatal distribution and size in southern Appalachian hardwoods. *Can J Bot* **53**, 1153–1156 (1975).
11. Brodribb, T. J. & Feild, T. S. Leaf hydraulic evolution led a surge in leaf photosynthetic capacity during early angiosperm diversification. *Ecol Lett* **13**, 175–183 (2010).
12. Carpenter, K. J. Stomatal architecture and evolution in basal angiosperms. *American Journal of Botany* **92**, 1595–1615 (2005).
13. Jordan, G. J., Carpenter, R. J., Koutoulis, A., Price, A. & Brodribb, T. J. Environmental adaptation in stomatal size independent of the effects of genome size. *New Phytologist* **205**, 608–617 (2015).
14. Scoffoni, C., Rawls, M., McKown, A., COCHARD, H. & Sack, L. Decline of Leaf Hydraulic Conductance with Dehydration: Relationship to Leaf Size and Venation Architecture. *Plant Physiology* **156**, 832–843 (2011).
15. Coomes, D. A., Heathcote, S., Godfrey, E. R., Shepherd, J. J. & Sack, L. Scaling of xylem vessels and veins within the leaves of oak species. *Biology Letters* **4**, 302–306 (2008).
16. de Boer, H. J. *et al.* Optimal allocation of leaf epidermal area for gas exchange. *New Phytologist* **210**, 1219–1228 (2016).
17. Delucia, E. H. & Berlyn, G. P. The effect of increasing elevation on leaf cuticle thickness and cuticular transpiration in balsam fir. *Can J Bot* **62**, 2423–2431 (1984).
18. Franks, P. J. & Beerling, D. J. CO<sub>2</sub>-forced evolution of plant gas exchange capacity and water-use efficiency over the Phanerozoic. *Geobiology* **7**, 227–236 (2009).

19. Gleason, S. M. *et al.* Weak coordination among petiole, leaf, vein, and gas-exchange traits across Australian angiosperm species and its possible implications. *Ecology and Evolution* **6**, 267–278 (2016).
20. Gola, E. M. & Szczesniak, E. in *Genus Polypodium L.* (eds. Szczesniak, E. & Gola, E. M.) 39–46 (Polish Botanical Society, 2012).
21. Haworth, M., Heath, J. & McElwain, J. C. Differences in the response sensitivity of stomatal index to atmospheric CO<sub>2</sub> among four genera of Cupressaceae conifers. *Ann Bot-London* **105**, 411–418 (2010).
22. Haworth, M., Fitzgerald, A. & McElwain, J. C. Cycads show no stomatal-density and index response to elevated carbon dioxide and subambient oxygen. *Aust J Bot* **59**, 630 (2011).
23. Haworth, M., Killi, D., Materassi, A. & Raschi, A. Coordination of stomatal physiological behavior and morphology with carbon dioxide determines stomatal control. *American Journal of Botany* **102**, 677–688 (2015).
24. Henry, T. A., Bainard, J. D., Newmaster, S. G. & Schwarzacher, T. Genome size evolution in Ontario ferns (Polypodiidae): evolutionary correlations with cell size, spore size, and habitat type and an absence of genome downsizing. *Genome* **57**, 555–566 (2014).
25. McElwain, J. C., Yiotis, C. & Lawson, T. Using modern plant trait relationships between observed and theoretical maximum stomatal conductance and vein density to examine patterns of plant macroevolution. *New Phytologist* **209**, 94–103 (2015).
26. Mehra, P. N. & Soni, S. L. Stomatal patterns in pteridophytes - an evolutionary approach. *Proceedings of the Indian National Science Academy* **B49**, 155–203 (1983).
27. Nardini, A., Gortan, E. & Salleo, S. Hydraulic efficiency of the leaf venation system in sun- and shade-adapted species. *Functional Plant Biol.* **32**, 953–961 (2005).
28. Nardini, A., Pedà, G. & Rocca, N. L. Trade-offs between leaf hydraulic capacity and drought vulnerability: morpho-anatomical bases, carbon costs and ecological consequences. *New Phytologist* **196**, 788–798 (2012).
29. Ogaya, R., Llorens, L. & Peñuelas, J. Density and length of stomatal and epidermal cells in “living fossil” trees grown under elevated CO<sub>2</sub> and a polar light regime. *Acta Oecologica* **37**, 381–385 (2011).
30. Pérez-Farrera, M. A., Vovides, A. P. & Avendaño, S. Morphology and Leaflet Anatomy of the Ceratozamia norstogii(Zamiaceae, Cycadales) Species Complex in Mexico with Comments on Relationships and Speciation. *Int J Plant Sci* **175**, 110–121 (2014).
31. Reed, J. E. & Smith, W. K. Stomatal Frequency, Distribution, and Needle Hydrophobicity in Cloud Forest Spruce and Fir, Southern Appalachian Mountains. *RURALS: Review of Undergraduate Research in Agricultural and Life Sciences* **7**, 1–12 (2012).
32. Sack, L. & Frole, K. Leaf structural diversity is related to hydraulic capacity in tropical rain forest trees. *Ecology* **87**, 483–491 (2006).
33. Tiwari, S. P., Kumar, P. & Yadav, D. Comparative morphological, epidermal, and anatomical studies of *Pinus roxburghii* needles at different altitudes in the North-West Indian Himalayas. *Turkish Journal of ...* **37**, 65–73 (2013).
34. Vovides, A. P., Etherington, J. R. & Dresser, P. Q. CAM-cycling in the cycad Dioon edule Lindl. in its natural tropical deciduous forest habitat in central Veracruz, Mexico. *Botanical Journal of ...* **138**, 155–162 (2002).

35. Wang, R. *et al.* Elevation-Related Variation in Leaf Stomatal Traits as a Function of Plant Functional Type: Evidence from Changbai Mountain, China. *PLoS ONE* **9**, e115395 (2014).
36. Zhang, S.-B. *et al.* Evolutionary Association of stomatal traits with leaf vein density in *Paphiopedilum*, Orchidaceae. *PLoS ONE* **7**, e40080 (2012).
37. Zwieniecki, M. A. & Boyce, C. K. Evolution of a unique anatomical precision in angiosperm leaf venation lifts constraints on vascular plant ecology. *P R Soc B* **281**, 20132829–20132829 (2014).
38. Colmer, T. D. & Pedersen O. Underwater photosynthesis and respiration in leaves of submerged wetland plants: gas films improve CO<sub>2</sub> and O<sub>2</sub> exchange. *New Phytologist* **177**, 918 - 926 (2008).
39. Plymale, E. L. & Wylie, R. B. The major veins of mesomorphic leaves. *American Journal of Botany* **31**, 99 - 106 (1944).
40. Sack, L., Scoffoni, C., McKown, A. D., Froel, K., Rawls, M., Havran J. C., Tran, H. & Tran, T. Developmentally based scaling of leaf venation architecture explains global ecological patterns. *Nature Communications* **3**, 837 (2012).
41. Feild, T. S., Upchurch, G. R., Chatelet, D. S., Brodribb, T. J., Grubbs, K. C., Samain, M-S. & Wanke S. Fossil evidence for low gas exchange capacities for early cretaceous angiosperm leaves. *Paleobiology* **37**, 195 - 213 (2016).
42. Weryszko-Chlewska, E. & Haratym, W. Leaf micromorphology of *Aesculus hippocastanum* L. and damage caused by leaf-mining larvae of *Cameraria ohridella* Deschka & Dimic. *Acta Agrobotanica* **65**, 25 - 34 (2012).
43. Brodribb, T. J., Jordan G. J. & Carpenter, R. J. Unified changes in cell size permit coordinated leaf evolution. *New Phytologist* **199**, 559 - 570 (2013).
44. Ekrt, L., Trávníček, P., Jarmolímová, V., Vít, P. & Urfus, T. Genome size and morphology of the *Dryopteris affinis* group in Central Europe. *Preslia* **81**, 261 - 280 (2009).
45. Jordan, G. J., Brodribb, T. J., Blackman, C. J. & Weston, P. H. Climate drives vein anatomy in Proteaceae. *American Journal of Botany* **100**, 1483 - 1493 (2013).
46. Walls, R. L. Angiosperm leaf vein patterns are linked to leaf functions in a global-scale data set. *American Journal of Botany* **98**, 244 - 253 (2011).
47. Darbyshire, S. J. & Francis, A. The biology of invasive alien plants in Canada. 10. *Nymphoides peltata* (S. G. Gmel.) Kuntze. *Canadian Journal of Plant Science* **88**, 811 - 829 (2008).
48. Fiorin, L. Spatial coordination between veins and stomata links water supply with water loss in leaves. PhD dissertation, University of Padova, January (2013).

## Article References

1. Friedman, W. E. The meaning of Darwin's "abominable mystery". *American Journal of Botany* **96**, 5–21 (2009).
2. Augusto, L., Davies, T. J., Delzon, S. & De Schrijver, A. The enigma of the rise of angiosperms: can we untie the knot? *Ecol Lett* **17**, 1326–1338 (2014).
3. Brodribb, T. J., Feild, T. S. & Jordan, G. J. Leaf Maximum Photosynthetic Rate and Venation Are Linked by Hydraulics. *Plant Physiology* **144**, 1890–1898 (2007).
4. Franks, P. J. & Beerling, D. J. Maximum leaf conductance driven by CO<sub>2</sub> effects on stomatal size and density over geologic time. *Proceedings of the National Academy of Sciences* **106**, 10343–10347 (2009).
5. Franks, P. J. & Farquhar, G. D. The effect of exogenous abscisic acid on stomatal development, stomatal mechanics, and leaf gas exchange in *Tradescantia virginiana*. *Plant Physiology* **125**, 935–942 (2001).
6. Sack, L. & Buckley, T. N. The developmental basis of stomatal density and flux. *Plant Physiology* **171**, 2358–2363 (2016).
7. de Boer, H. J. *et al.* Optimal allocation of leaf epidermal area for gas exchange. *New Phytologist* **210**, 1219–1228 (2016).
8. John, G. P., Scoffoni, C. & Sack, L. Allometry of cells and tissues within leaves. *American Journal of Botany* **100**, 1936–1948 (2013).
9. de Boer, H. J., Eppinga, M. B., Wassen, M. J. & Dekker, S. C. A critical transition in leaf evolution facilitated the Cretaceous angiosperm revolution. *Nature Communications* **3**, 1–11 (2012).
10. Carins Murphy, M. R., Jordan, G. J. & Brodribb, T. J. Differential leaf expansion can enable hydraulic acclimation to sun and shade. *Plant Cell Environ* **35**, 1407–1418 (2012).
11. Feild, T. S. & Brodribb, T. J. Hydraulic tuning of vein cell microstructure in the evolution of angiosperm venation networks. *New Phytologist* **199**, 720–726 (2013).
12. Mirsky, A. E. & Ris, H. The desoxyribonucleic acid content of animal cells and its evolutionary significance. *J. Gen. Physiol.* **34**, 451–462 (1951).
13. Cavalier-Smith, T. Nuclear volume control by nucleoskeletal DNA, selection for cell volume and cell growth rate, and the solution of the DNA C-value paradox. *J Cell Sci* **34**, 247–278 (1978).
14. Simova, I. & Herben, T. Geometrical constraints in the scaling relationships between genome size, cell size and cell cycle length in herbaceous plants. *P R Soc B* **279**, 867–875 (2012).
15. Beaulieu, J. M., Leitch, I. J., Patel, S., Pendharkar, A. & Knight, C. A. Genome size is a strong predictor of cell size and stomatal density in angiosperms. *New Phytologist* **179**, 975–986 (2008).
16. Leitch, I. J. Evolution of DNA Amounts Across Land Plants (Embryophyta). *Ann Bot-London* **95**, 207–217 (2005).
17. Jiao, Y. *et al.* Ancestral polyploidy in seed plants and angiosperms. *Nature* **473**, 97–100 (2011).
18. Bennett, M. D. Nuclear DNA content and minimum generation time in herbaceous plants. *Proc. R. Soc. Lond., B, Biol. Sci.* **181**, 109–135 (1972).
19. Bennett, M. D. Variation in genomic form in plants and its ecological implications. *New Phytologist* **106**, 177–200 (1987).
20. Hodgson, J. G. *et al.* Stomatal vs. genome size in angiosperms: the somatic tail wagging

- the genomic dog? *Ann Bot-London* **105**, 573–584 (2010).
21. Franks, P. J., Freckleton, R. P., Beaulieu, J. M., Leitch, I. J. & Beerling, D. J. Megacycles of atmospheric carbon dioxide concentration correlate with fossil plant genome size. *Philos T R Soc B* **367**, 556–564 (2012).
22. *Plant DNA C-values database*. (kew, 2012). Available at: <http://data.kew.org/cvalues/>. (Accessed: 15 February 2017)
23. Smith, J. & Winter, K. in *Crassulacean Acid Metabolism Biochemistry, Ecophysiology and Evolution* (eds. Winter, K. & Smith, A. J.) 427–436 (Crassulacean acid metabolism, 1996).
24. Franks, P. J. & Farquhar, G. D. The mechanical diversity of stomata and its significance in gas-exchange control. *Plant Physiology* **143**, 78–87 (2007).
25. Simonin, K. A., Limm, E. B. & Dawson, T. E. Hydraulic conductance of leaves correlates with leaf lifespan: implications for lifetime carbon gain. *New Phytologist* **193**, 939–947 (2012).
26. Magallón, S., Gómez-Acevedo, S., Sánchez-Reyes, L. L. & Hernández-Hernández, T. A metacalibrated time-tree documents the early rise of flowering plant phylogenetic diversity. *New Phytologist* **207**, 437–453 (2015).
27. Lu, Y., Ran, J.-H., Guo, D.-M., Yang, Z.-Y. & Wang, X.-Q. Phylogeny and Divergence Times of Gymnosperms Inferred from Single-Copy Nuclear Genes. *PLoS ONE* **9**, e107679 (2014).
28. Testo, W. & Sundue, M. Molecular Phylogenetics and Evolution. *Molecular Phylogenetics and Evolution* **105**, 200–211 (2016).
29. Magallon, S., Hilu, K. W. & Quandt, D. Land plant evolutionary timeline: Gene effects are secondary to fossil constraints in relaxed clock estimation of age and substitution rates. *American Journal of Botany* **100**, 556–573 (2013).
30. Brodribb, T. J. & Feild, T. S. Leaf hydraulic evolution led a surge in leaf photosynthetic capacity during early angiosperm diversification. *Ecol Lett* **13**, 175–183 (2010).
31. Webb, C. O., Ackerly, D. D. & Kembel, S. W. Phylocom: software for the analysis of phylogenetic community structure and trait evolution. *Bioinformatics* **24**, 2098–2100 (2008).
32. Huelsenbeck, J. P., Nielsen, R. & Bollback, J. P. Stochastic Mapping of Morphological Characters. *Systematic Biology* **52**, 131–158 (2003).
33. Revell, L. J. phytools: an R package for phylogenetic comparative biology (and other things). *Methods Ecol Evol* **3**, 217–223 (2011).
34. Paradis, E., Claude, J. & Strimmer, K. APE: Analyses of Phylogenetics and Evolution in R language. *Bioinformatics* **20**, 289–290 (2004).
35. Feild, T., Brodribb, T. & Iglesias, A. Fossil evidence for Cretaceous escalation in angiosperm leaf vein evolution. *Proceedings of the National Academy of Sciences* **108**, 8363–8366 (2011).
36. Kembel, S. W. et al. Picante: R tools for integrating phylogenies and ecology. *Bioinformatics* **26**, 1463–1464 (2010).
37. Clavel, J., Escarguel, G. & Merceron, G. mv morph: an rpackage for fitting multivariate evolutionary models to morphometric data. *Methods Ecol Evol* **6**, 1311–1319 (2015).
38. Franks, P. J., Leitch, I. J., Ruszala, E. M., Hetherington, A. M. & Beerling, D. J. Physiological framework for adaptation of stomata to CO<sub>2</sub> from glacial to future concentrations. *Philos T R Soc B* **367**, 537–546 (2012).

39. Coomes, D. A., Heathcote, S., Godfrey, E. R., Shepherd, J. J. & Sack, L. Scaling of xylem vessels and veins within the leaves of oak species. *Biology Letters* **4**, 302–306 (2008).
40. Pittermann, J., Sperry, J., Hacke, U., Wheeler, J. & Sikkema, E. Torus-Margo Pits Help Conifers Compete with Angiosperms. *Science* **310**, 1924–1924 (2005).
41. Boyce, C. K. & Lee, J.-E. Could Land Plant Evolution Have Fed the Marine Revolution? *Paleontological Research* **15**, 100–105 (2011).
42. Boyce, C. K., Brodribb, T. J., Feild, T. S. & Zwieniecki, M. A. Angiosperm leaf vein evolution was physiologically and environmentally transformative. *P R Soc B* **276**, 1771–1776 (2009).
43. Sanderson, M. J. & Donoghue, M. J. Shifts in diversification rate with the origin of angiosperms. *Science* **264**, 1590–1593 (1994).
44. Labandeira, C. C. & Currano, E. D. The Fossil Record of Plant-Insect Dynamics. *Annu Rev Earth Pl Sc* **41**, 287–311 (2013).
45. Crepet, W. L. & Niklas, K. J. Darwin's second “abominable mystery”: Why are there so many angiosperm species? *American Journal of Botany* **96**, 366–381 (2009).
46. Fenster, C. B., Armbruster, W. S., Wilson, P., Dudash, M. R. & Thomson, J. D. Pollination Syndromes and Floral Specialization. *Annu Rev Ecol Evol S* **35**, 375–403 (2004).
47. Labandeira, C. C., Dilcher, D. L., Davis, D. R. & Wagner, D. L. Ninety-seven million years of angiosperm-insect association: paleobiological insights into the meaning of coevolution. *P Natl Acad Sci Usa* **91**, 12278–12282 (1994).
48. Berendse, F. & Scheffer, M. The angiosperm radiation revisited, an ecological explanation for Darwin's ‘abominable mystery’. *Ecol Lett* **12**, 865–872 (2009).
49. Ehleringer, J. R. & Monson, R. K. Evolutionary and ecological aspects of photosynthetic pathway variation. *Annual Review of Ecology and Evolution* **24**, 411–439 (1993).